New York Science Journal

Websites:
http://www.sciencepub.net/newyork
http://www.sciencepub.net

Emails:
newyorksci@gmail.com
editor@sciencepub.net

MARSLAND PRESS
Multidisciplinary Academic Journal Publisher

Assessment of porosity of glass-ionomer cement using ultrasonic waves

Touriya BASSIDI, Lahcen MOUNTASSIR, Hassan NOUNAH, Khalid BOUABID

Laboratory of Metrology and Information Processing, Faculty of Science, Ibn Zohr University, Agadir, Morocco
† t.bassidi@gmail.com

Abstract
The goal of this study was to investigate the relationship between porosity and ultrasonic parameters of glass-ionomer dental cement. Theoretical Schoch model describing the ultrasonic propagation in materials was proposed. Ultrasonic velocities and mechanical properties were evaluated. They were then, compared to the experimental ultrasonic parameters measured on dry and saturated samples with varying porosity. As expected, a linear decrease of ultrasonic velocities versus porosity is observed for two saturation states. The correlation between theoretical and measured results is analyzed. The Schoch model succeeded in describing the acoustic parameters in dry and saturated state.
[Touriya BASSIDI, Lahcen MOUNTASSIR, Hassan NOUNAH, Khalid BOUABID. **Assessment of porosity of glass-ionomer cement using ultrasonic waves .** *N Y Sci J* 2023;16(10):71-82]. ISSN 1554-0200 (print); ISSN 2375-723X (online). http://www.sciencepub.net/newyork. 02.doi:10.7537/marsnys161023.02.

Keywords: Glass-ionomer cement, Mechanical properties, porosity, Ultrasound.

Introduction

Glass ionomer cements (GICs) are widely utilized in a variety of different applications in dentistry, from luting cements to following filling materials. Their main advantages are good adhesion to tooth enamel and dentin,[1,2] good esthetics [3], acceptable handling properties, do not undergo polymerization shrinkage [4] and ability to release fluoride [5,6]. However, the low mechanical properties of these materials prevent their applications in larger dental care, particularly in occlusal restoration [7-9].

Since the introduction of GICs in the early 1970 s [10] the cements have generally been formed by an acid–base reaction between the acidic liquid and basic glass powder. When the polyalkenoic acid and the glass powder are combined, the hydrogen ions of the polyacid attack and degrade the glass structure, and then calcium and aluminium cations are released from the glass. These cations combine with the carboxylate groups of polyalkenoic acid to form the polysalt matrix, and the cement hardens [11-14].

The resin modified GICs (RMGIs) have been introduced by adding resin components to conventional GIGs to improve their mechanical properties. However, these materials have some of the disadvantages due to use of resins, toxicological problem and polymerization shrinkage. The RMGIs have poorer long-term mechanical properties and inferior bio- compatibility compared to conventional GICs [15-18].

Many Studies have already analyzed the mechanical properties of GI. The mechanical strength of GIC is widely influenced by the numbers of parameters, such as the mixing technique [19-22], the powder to liquid ratio [23], the presence of surface flaws [24] and the total porosity [25-27]. Wiming et al. [28-29] suggested that the compressive strength and elastic modulus are dependent on the concentration and molar mass of the polyacid in the GIC that have. These results indicate that the microstructure of GIC plays an important role in their mechanical properties.

Ultrasonic imaging is a valuable tool in nondestructive methods. Ultrasonic devices are also used for evaluating the microstructure and the mechanical properties of materials [30-32]. Because the acoustic parameters such as longitudinal and shear wave velocity are strongly correlated to the viscoelastic properties of materials [33]. The characteristics of dental materials can therefore be determined by measuring the ultrasonic speeds within a specimen.

The aim of this study was to evaluate the porosity in cured cement samples and investigate their influence on the mechanical properties using the ultrasonic device. The technique used is based on measurement of the variations of the ultrasonic properties, as a function of porosity. Then, the mechanical properties of GICs are deduced for each porosity rate. Acoustic wave propagation in GICs was experimentally and theoretically investigated. For a theoretical estimation, the Schoch model was employed. The experimental measurement showed good correlation with the theoretical estimates.

Theoretical model

Schoch [34] has proposed a simple model describing acoustic wave propagation in non-porous media materials which are homogeneous and isotropic. This simulation allows to predict the reflection coefficient at the interface between coupling liquid and materials fig.1.

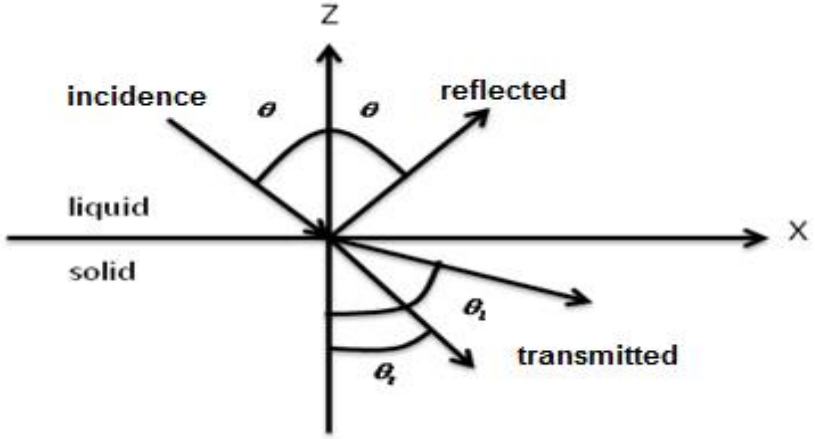

Fig.1 Problem geometry

The reflection coefficient is defined as the ratio between the amplitude of reflected wave and incident wave. It is written as a function of incident angle, as [35]:

$$R_S(\theta) = \frac{Z_l cos^2 2\theta_t + Z_l sin^2 2\theta_t - Z_{liq}}{Z_l cos^2 2\theta_t + Z_l sin^2 2\theta_t + Z_{liq}} \quad (1)$$

with Z_{liq} , Z_l and Z_t are the acoustic impedance for coupling liquid, the longitudinal and the transversal acoustic impedance for the material.

However, to apply this model to the case of our porous structures, require making some changes in the acoustics parameters, in order to introduce the porosity.

Phani and Maitra [36-37] have been proposed a theoretical relationship between ultrasonic parameters and material microstructure which take into account the morphology of the pore and is valid for all porosity values. The longitudinal velocity V_l is related to porosity ϕ by following formula [38]:

$$V_l = V_{l0}(1-\phi)^P \quad (2)$$

Where V_{l0} is the longitudinal wave velocity at zero porosity (in the following, index '0' refers to zero porosity in material), and p is empirical constant that depends on the pore morphology. For a medium saturated with a fluid, the equation of Phani is modified to take into account the saturating fluid velocity V_f [39]. Then, the equation becomes [38]:

$$V_l = V_{l0}(1-\phi)^m + \phi V_f \quad (3)$$

As fluids do not support shear stresses, the transverse velocity V_t is related to the porosity by the expression:

$$V_t = V_{t0}(1-\phi)^s \quad (4)$$

The parameters m and s depend on the pores' geometry [38]. The values of s and m are 1 for cylindrical pores and 0.5 for spherical pores.

The density of saturated porous material ρ_p is related to the porosity by the following expression:

$$\rho_p = \rho_0(1-\phi) + \phi\rho_f \quad (5)$$

where ρ_f is the density of saturating fluid.

The acoustic parameters and densities of materials studied in this study are presented in table1.

Table 1 Acoustic properties of glass-ionomer cement, water and air

	Density ρ(Kg/m^3)	longitudinal velocity V_l (m/s)	Transversal velocity V_t (m/s)
Glass-ionomer cement	2050	3670	1930
Water	1000	1500	-
Air	1	300	-

Materials and methods

The restorative glass ionomer cement used in this study was Fuji II (). The glass ionomer was hand mixed, in accordance with the manufacturer's instructions. A paper pad and stainless steel spatula were used for hand mixing. After mixing time, the specimens were placed in cylindrical molds, 1cm in diameter and 0.23 cm in height. One hour after the completion of hardening, the hardened samples were removed from the molds and used in the investigation. The density of each sample was determined from the mass and a total volume. The size of each sample was measured using a digital caliper (precision: 0.01 mm) to determine the total volume. The mass was measured using an analytical balance (precision: 0.001 g). The density ρ is the ratio between the mass and volume using the following formula:

$$\rho = \frac{m}{V} \tag{6}$$

Porosity was measured using gravity method. The samples were immersed in water until they are fully saturated. Then, they are weighted with precision. Porosity p is determined using the following expression.

$$p = \frac{M_{sat} - M_{dry}}{\rho_w V_{vol}} \tag{7}$$

where M_{dry} and M_{sat} they are respectively weight of dried and saturated sample, ρ_w is the volume density of water and V_{vol} is the volume of the sample.

The ultrasound reflectivity at normal incidence was used in this study to measure the longitudinal wave speeds. The ultrasound device comprised a pulse generator (SOFRANEL model 5052PR), transducer (Panametrics V309, piezoelectric circular with 7.06 mm in diameter and 5 MHz as central frequency) that plays as an emitter and receiver at the same time and a picoscope PC oscilloscope that connected to a computer. The pulse generator excites the transducer for transmitting and receiving an ultrasound signal. The transducer that was perpendicular to the surface of contact of the specimen. The ultrasonic wave was sent by the transducer to the specimen and then reflected off by the surfaces of the sample and received by the same transducer. The generator is connected to a picoscope to acquire the backscattered. The signal received by a picoscope is retrieved on a computer.

Two saturation states of each sample were tested, dry and water saturated. Water saturation of samples was performed by immersing specimens in distilled water for 24 hours. For dry specimens, instead of the immersion coupling, a thin layer of coupling agent (silicone gel) is applied to the transducer/dry sample to prevent penetration of water into the sample during the ultrasonic measurement.

The time differential Δt (fig. 2) between the echoes reflected by the two surfaces of specimen represented the flight time required for the wave to propagate through the samples. The sound velocity V was calculated by measuring Δt and the specimen thickness e, as shown in the following formula:

$$V = \frac{2e}{\Delta t} \tag{8}$$

Acoustic waves that propagate in a porous material are directly related to its mechanical properties. The characteristics of Glass-ionomer cement can therefore be determined by measuring the V_l and V_t within a specimen and using the well-known relations [40-41].

$$E = \rho V_t^2 \left(\frac{3V_l^2 - 4V_t^2}{V_l^2 - V_t^2} \right) \quad (9)$$

$$G = \frac{E}{2(1+\nu)} \quad (10)$$

where E and G are respectively the Young's and shear modulus.

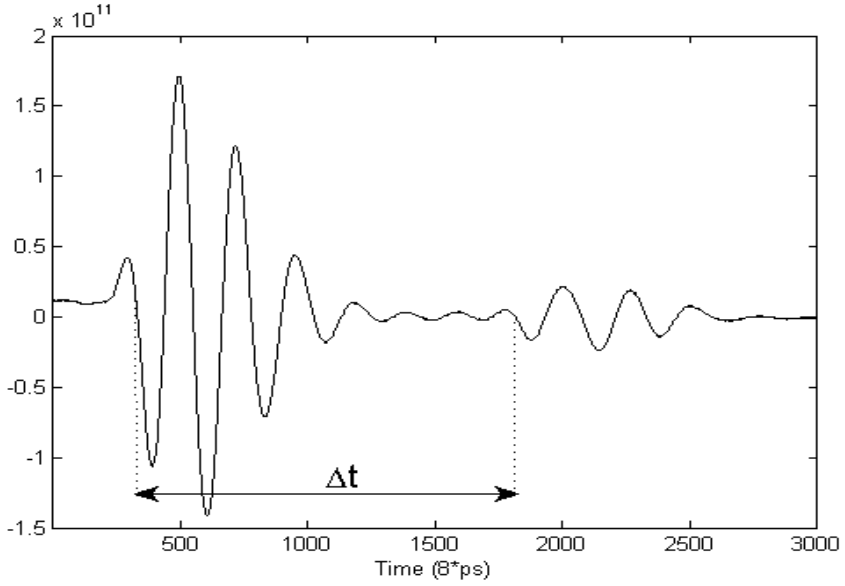

Fig. 2 Measurement of pulse velocity, reflected pulses and estimation of time delay Δt

Results and discussions

Model prediction

Fig. 3 shows the estimated amplitude and phase of the reflectivity at the interface between water and porous GIC as a function of the incident angle. Longitudinal, transversal and Rayleigh velocities are measured using the following formulas:

$$V_L = \frac{V_{water}}{sin\theta_{cl}}, \quad V_T = \frac{V_{water}}{sin\theta_{ct}}, \quad V_R = \frac{V_{water}}{sin\theta_{cR}}$$

Where (θ_{cl}), (θ_{ct}) and (θ_{cR}) are respectively critical angle of longitudinal, transversal and Rayleigh wave. The variation of longitudinal V_l, shear V_t and Rayleigh V_R wave velocity with porosity for two saturation cases s presented in figs.4. It may be seen that the longitudinal velocity is affected by both porosity and saturation fluid. A significant decrease of this velocity with increasing porosity is observed. For a given porosity level, the value of longitudinal speed in water saturated case is higher than in the dry case. Ohdaira et al. [43] are confirmed that the presence of water within the pore increased stiffness when compare the dry and saturated material.

As expected, the behavior of shear and Rayleigh wave velocity is similar to that of longitudinal wave velocity. However, the shear wave is not affected by the fluid saturation (is not propagating in fluids). The Rayleigh wave corresponds to the superposition of longitudinal and transverse motions. Because the shear wave much more important role in the propagation of this wave, the Rayleigh wave appears less sensitive to fluid saturation. The longitudinal ultrasonic velocity is more sensitive to porosity in the material. This is coherent with the studies [42] based on the premise that the ultrasonic longitudinal velocity is more sensitive to changes in the microstructure of materials.

The same the mechanical properties of GIC versus porosity were estimated and were presented in fig.5. In it can be seen that all properties decrease with increasing porosity. On average, the values for saturated state are 6% higher than those for the dry state.

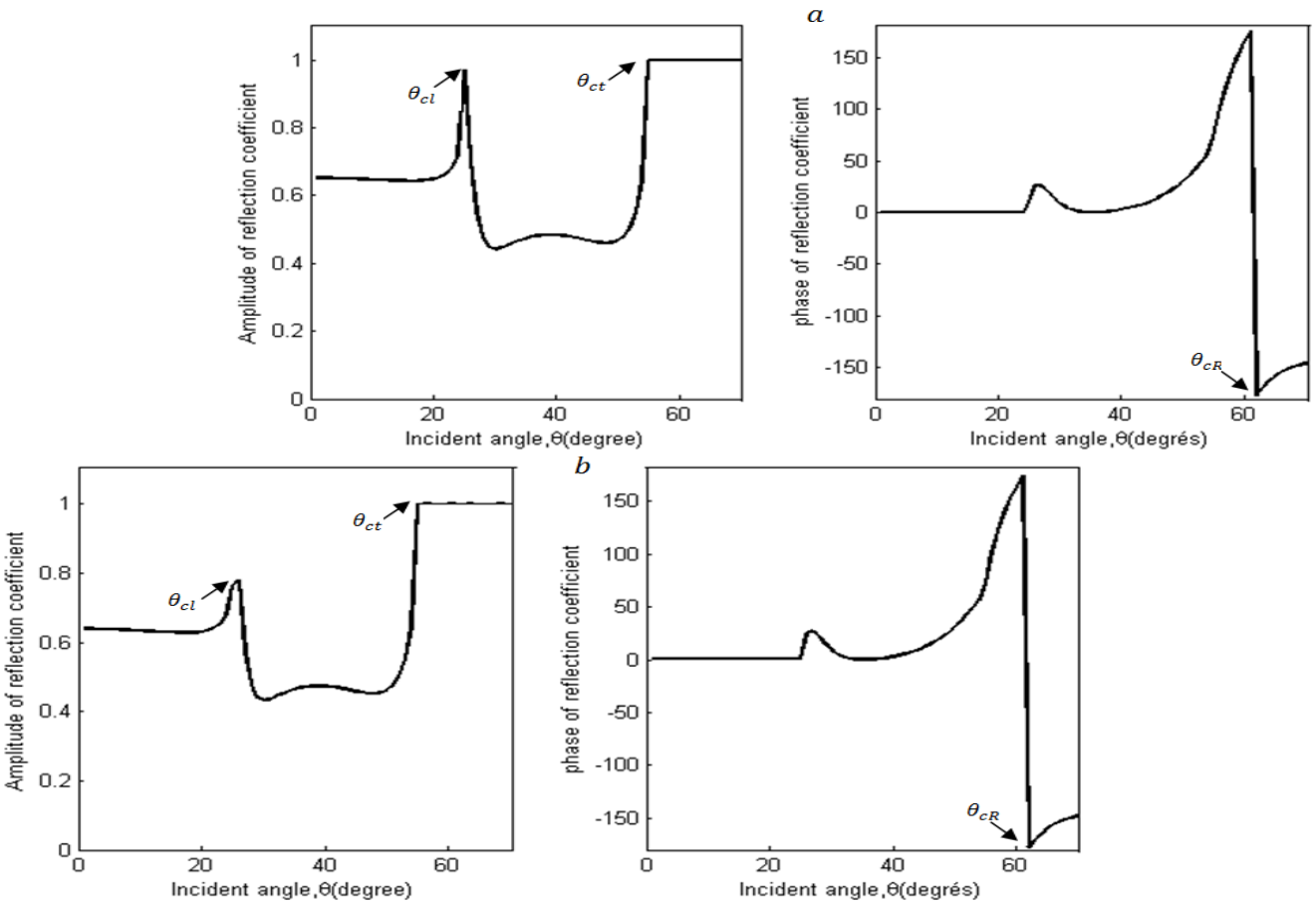

Fig. 3. Amplitude and phase of the reflection coefficient of GIC plate for $\phi = 5\%$. Saturated (a), dry (b)

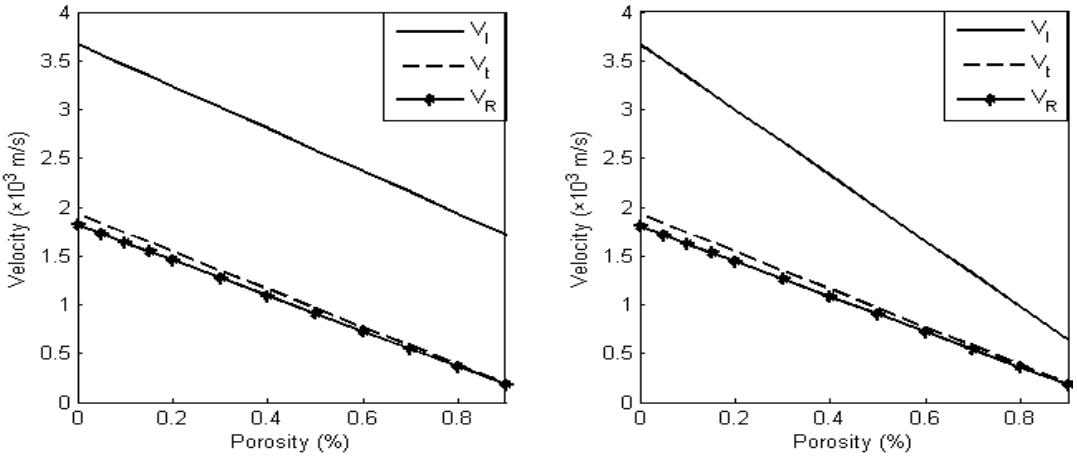

Fig. 4. Ultrasonic velocities for two saturation states versus porosity. Saturated (right), dry (lift)

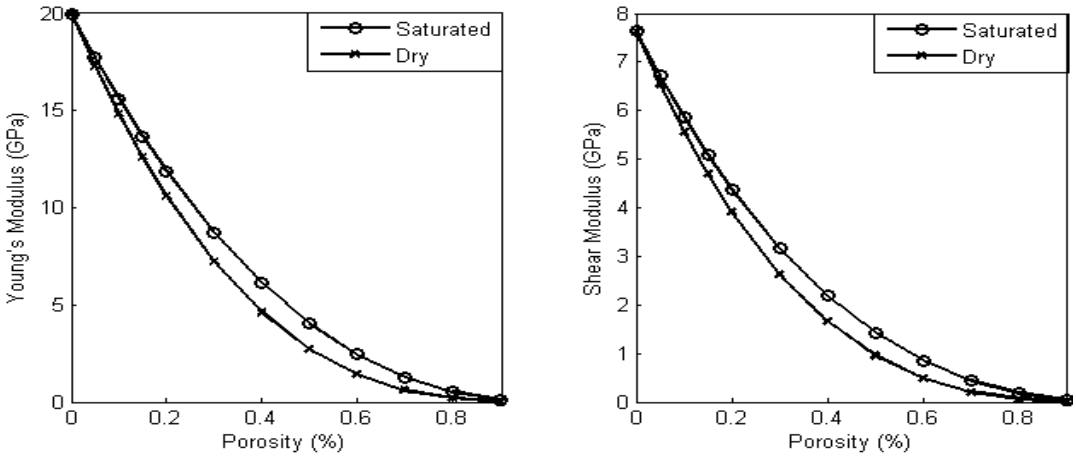

Fig. 4. Ultrasonic velocities for two saturation states versus porosity. Saturated (right), dry (lift)

Experimental results

In order to evaluate experimentally the effect of porosity on ultrasonic parameters, five samples of GIC were submitted to the two tests set out in section 3: porosity and pulse velocity measurement. Various levels of porosity were obtained each time we hand mixed and formed the samples in the moulds. For each saturation cases, the presented result is the mean value of the replicate measurements carried out on the GIC samples

Table 2 displays the measured longitudinal velocity versus porosity, for dry and water saturated specimens. It is found that the velocity depends strongly on the porosity and fluid saturation. As observed in the model calculation, the measured results also show the velocity decrease with increasing porosity. For a given value of porosity($p = 14.93\%$), v_l decreases from $3270\mathrm{m/s}$ for water-saturated state to $3150\mathrm{m/s}$ for dry state. This trend is coherent with the model.

Measurement of the shear wave speed creates substantial difficulties that the transduction of this wave through the material requires a good contact between the transducer and the porous material. This leads to the infiltration of the coupling agent in the pores. To overcome this problem, we were approximately determined the transverse speed using the following formula:

$$V_t = \frac{V_l}{2} \quad (11)$$

The Rayleigh wave velocity was determined using the relationship Victorov [44], [45]:

$$V_R = V_t \frac{0.718 - \left(V_t/V_l\right)^2}{0.750 - \left(V_t/V_l\right)^2} \quad (12)$$

Table 2 Experimental density and longitudinal velocity for dry and saturated cement versus porosity

Samples	Density (Kg/m^3)	Porosity	Water saturated		Air saturated	
			longitudinal velocity (m/s)	Relative Error	Longitudinal velocity (m/s)	Relative Error
1	2176	0.0	3750	4.8%	3706	4.0%
2	2048	0. 0525	3493	4.2%	3410	4.0%
3	1942.3	0.0975	3382	2.4%	3326	2.5%
4	1798	0.123	3300	5.0%	3320	3.5%
5	1744.1	0.1493	3270	5.5%	3150	2.9%

Correlation

Fig.6 shows a comparison between the measured and estimated evolution of longitudinal wave velocity with porosity for the considered two saturation states. To evaluate the agreement of experimental data with the model, a linear regression is performed on the curves presented on fig.6. The correlation coefficient is presented in this figure. All values of the regression coefficient R are found to be higher than 0.98, which means that the Schoch model correctly describes the variation of UPV with porosity.

Figs.7, 8 and 9 show the evolution of dynamic elastic parameters- transversal wave velocity, Young's and shear modulus with porosity. These parameters are derived from measured l-wave velocity using eqs (9), (10) and (11). A good linear correlation between all properties and porosity is observed. Comparison of measured data with the model demonstrates a very good agreement. In both figs, the correlation coefficient R is presented. All values are found to be higher than 0.96. This means that the experimental results fit well with the model.

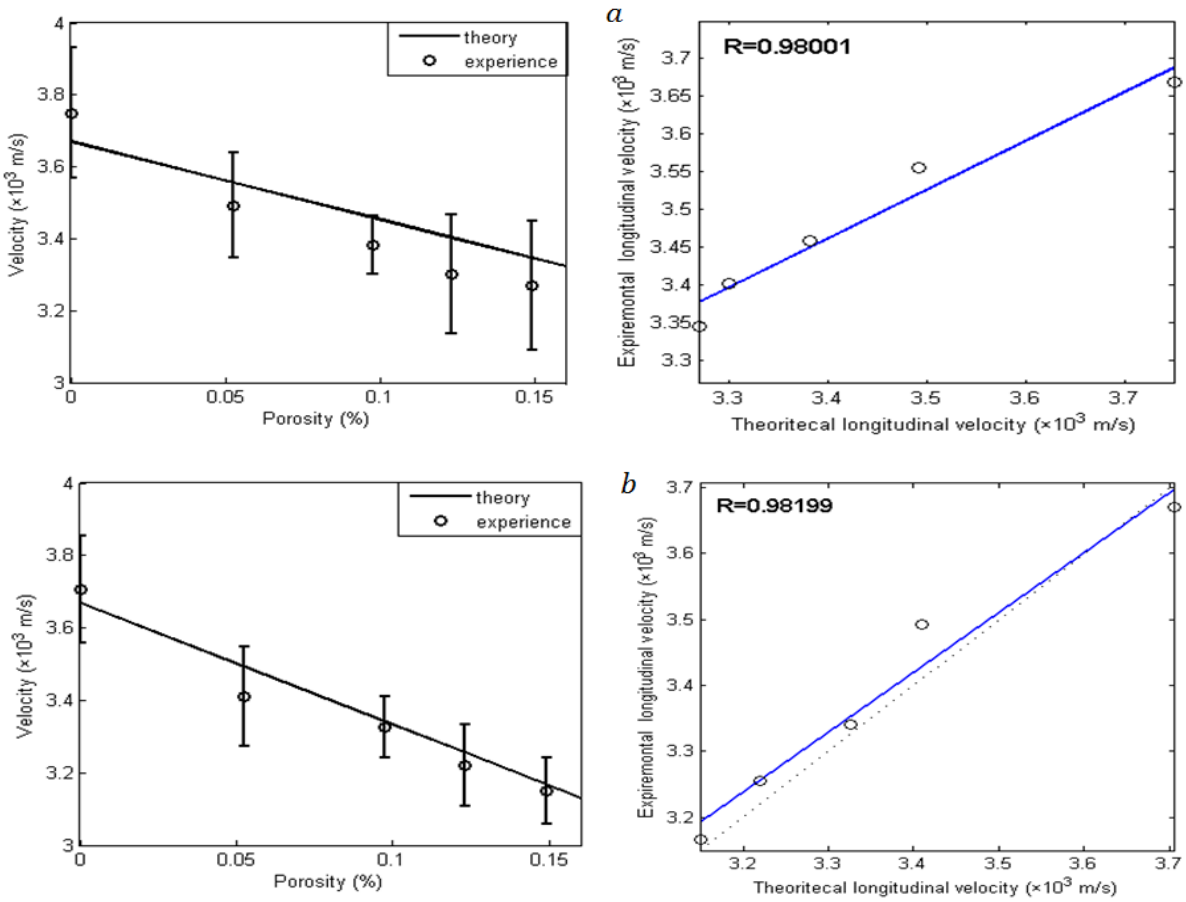

Fig. 6. Experimental and theoretical longitudinal velocity for GIC plate versus porosity. Saturated (a), dry (b)

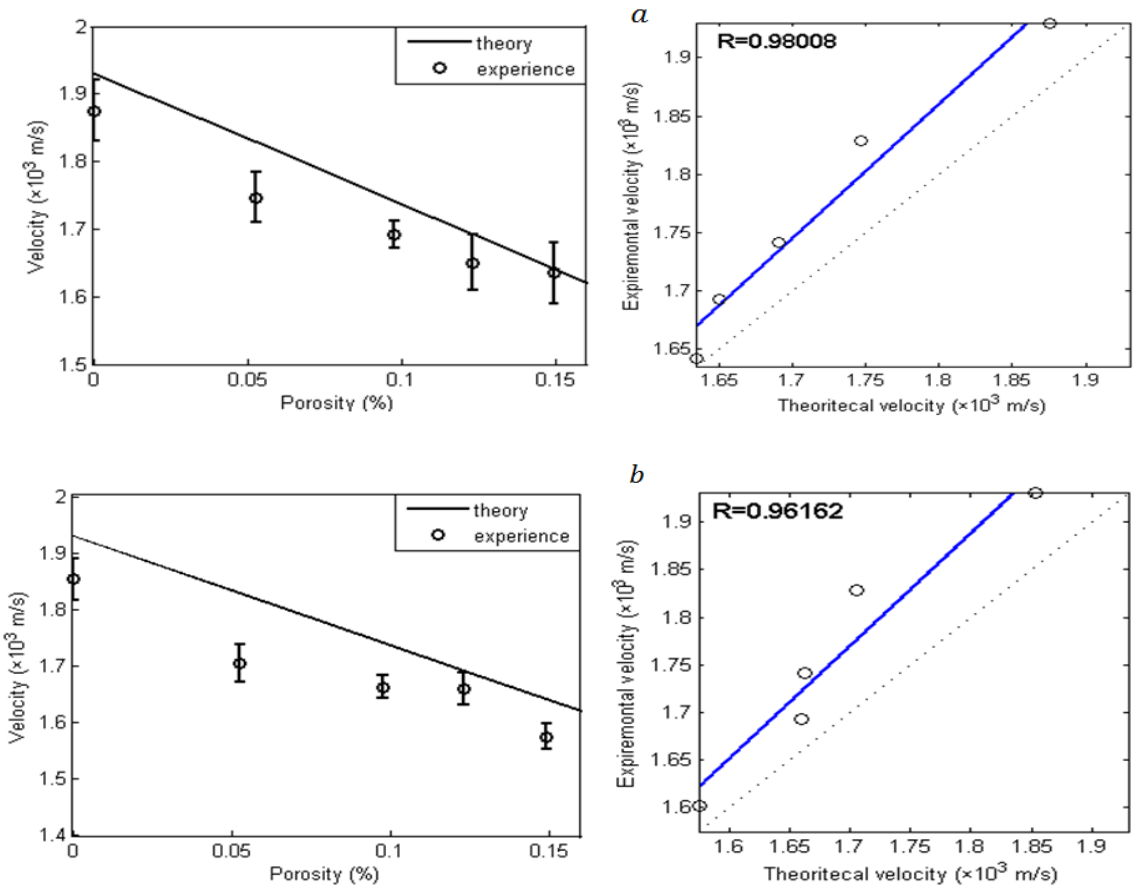

Fig.7. Experimental and theoretical shear velocity for GIC plate versus porosity. Saturated (a), dry (b)

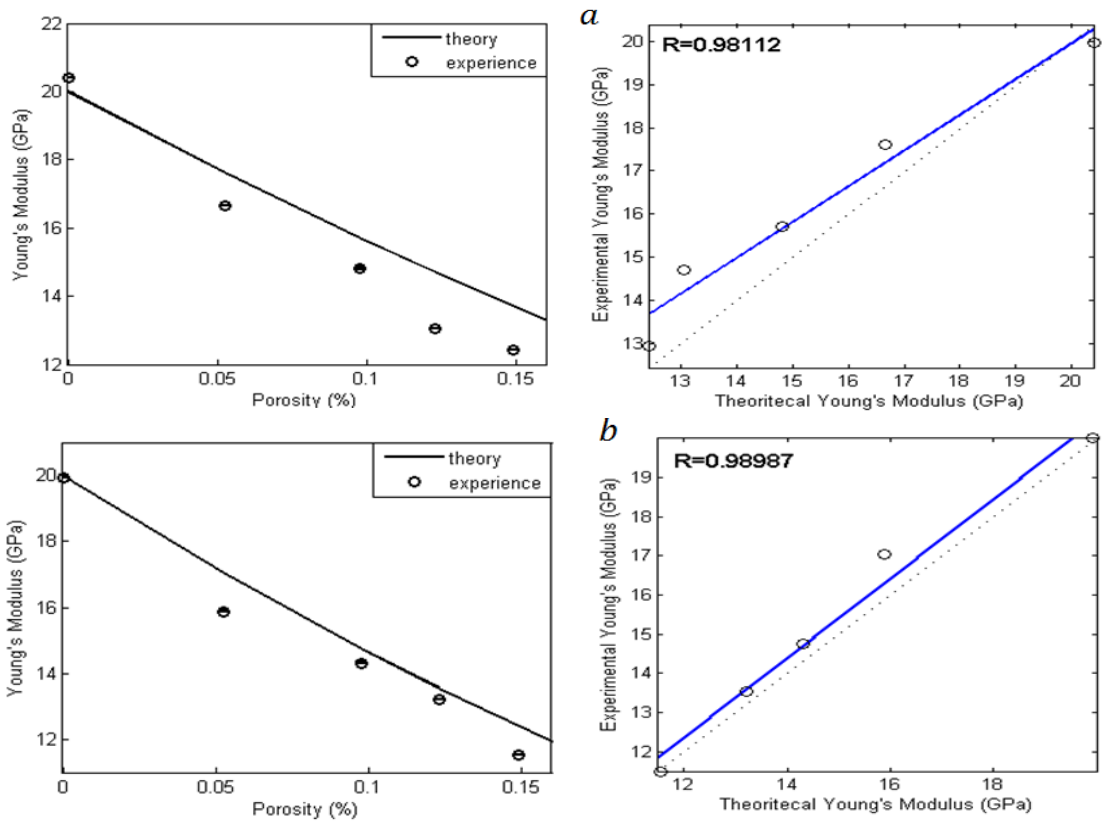

Fig. 8. Experimental and theoretical Young's modulus for GIC plate versus porosity. Saturated (a), dry (b)

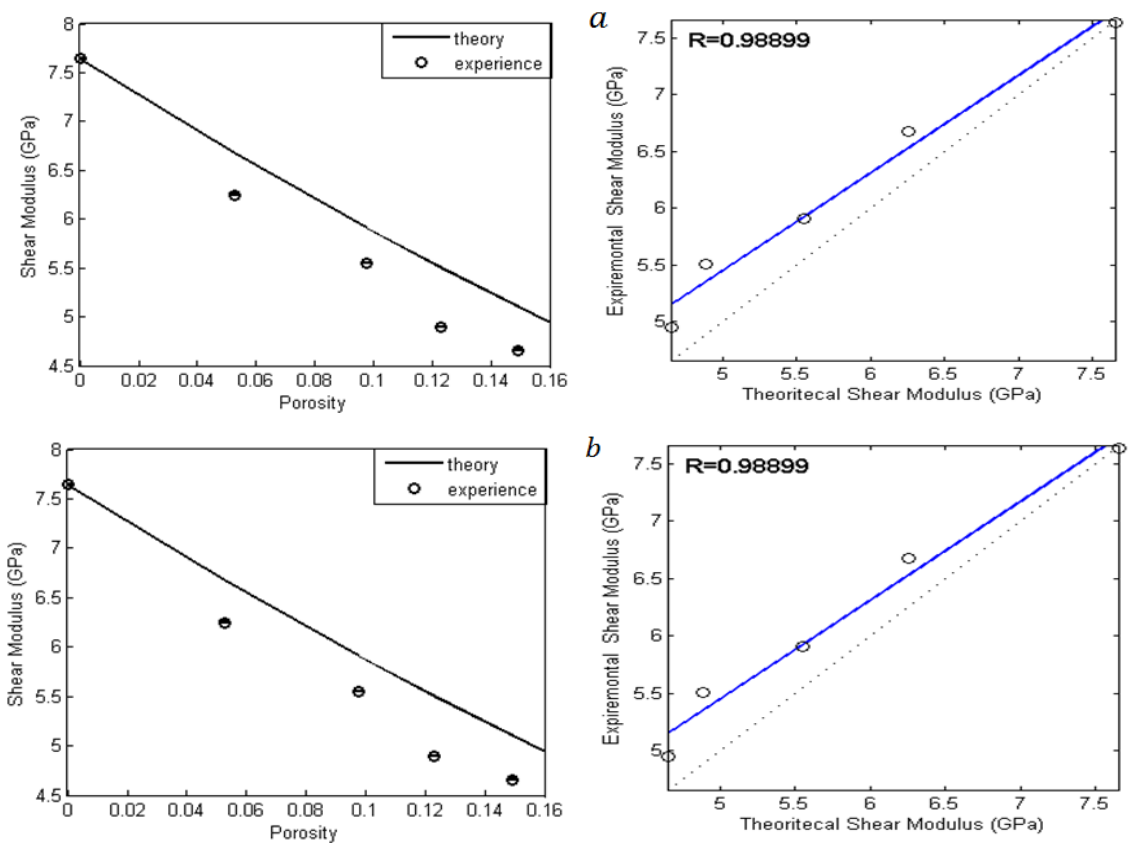

Fig. 9 Experimental and theoretical shear modulus for GIC plate versus porosity. Saturated (a), dry (b)

Conclusion

In this paper, the relationship between ultrasonic parameters and porosity in dry and fully saturated GI dental cement paste was investigated through Schoch modeling and comparison with experimental measurement. This model reported in the literature to study the propagation of acoustic waves in materials. The results obtained are as follows:

- Both longitudinal and transverse velocities decrease with porosity.
- The longitudinal pulse velocity increases with the water content in the pores while the shear wave velocity is not affected by the fluid of saturation. The longitudinal wave is more sensitive to change in microstructure of cement paste
- The Schoch model generally underestimates the measured ultrasonic velocities and both dry and saturated states of the Glass-ionomer cement paste

The determination of these velocities led to predict the mechanical properties

References

[1] Smith DC. Polyacrylic acid-based cements—adhesion to enamel and dentin. Oper Dent 1992;177—83.
[2] Erickson RL, Glasspoole EA. Bonding to tooth structure: a comparison of glass-ionomer and composite—resin systems. J Esthet Dent 1994;6:227—44.
[3] Asmussen E. Opacity of glass-ionomer cements. Acta Odontol Scand 1983;41:155—7.
[4] Brook IM, Hatton PV. Glass-ionomers: bioactive implantmaterials. Biomaterials 1998;19:565–71.
[5] Mitra SB. In vitro fluoride release from a light-cured glassionomer liner base. J Dent Res 1991;70:75—8.
[6] Forss H. Release of fluoride and other elements from lightcured glass ionomers in neutral and acidic conditions. J Dent Res 1993;72:1257—62.))
[7] Bowen RL, Marjenhoff WA. Dental composites/glassionomers: the materials. Adv Dent Res 1992;6:44–9.
[8] Sidhu SK. Glass-ionomer cement restorative materials: asticky subject? Aust Dent J 2011;56(Suppl. 1):23–30.
[9] Frencken JE. The ART approach using glass-ionomers inrelation to global oral health care. Dent Mater 2010;26:1–6).(**Effect of immersion time of restorative glassionomer cements and immersion duration incalcium chloride solution on surface hardness**

[10] Wilson AD. The chemistry of dental cements. Chem Soc Rev 1978;7:265–96.
[11] Wasson EA, Nicholson JW. New aspects of the setting of glass-ionomer cements. J Dent Re 1993;72:481-3.. Matsuya S, Maeda T, [12] Ohta M. IR and NMR analyses of hardening and maturation of glass-ionomer cement. J Dent Res 1996;75:1920-7.
[13] Wilson AD, Nicholson JW. Acid-Base Cements: Their Biomedical and Industrial Applications. Cambridge England.New York, NY, USA: Cambridge University Press; 1993
[14] Nicholson JW. Chemistry of glass-ionomer cements: areview. Biomaterials 1998;19:485–94
[15] AnsticeHM,NicholsonJW.Studiesonthestructureof light-cured glass-ionomer cements. J Mater Sci-Mater Med 1992;3:447—51.
[16] Kanchanavasita W, Anstice HM, Pearson GJ. Long-term surface micro-hardness of resin-modified glass ionomers. J Dent 1998;26:707-12.
[17] Cattani-Lorente MA, Dupuis V, Payan J, Moya F, Meyer JM. Effect of water on the physical properties of resin-modified glass ionomer cements. Dent Mater 1999;15:71—8.
[18] Nicholson JW,CzarneckaB.Biocompatibilityofresin-modified glass-ionomer dental cements.DentMater2008;24:1702–8.
[19] Fleming, G. J. & Zala, D. M. An assessment of encapsulated versus hand-mixed glass ionomer restoratives. Oper. Dent. 28, 168–177 (2003).
[20] Nomoto, R.&McCabe, J. F. Effect of mixing methods on the compressive strength of glass ionomer cements. J. Dent. 29, 205–210 (2001).
[21]. Dowling, A. H. & Fleming, G. J. Is encapsulation of posterior glass-ionomer restoratives the solution to clinically induced variability introduced on mixing? Dent. Mater. 24, 957–966 (2008).
[22] Dowling, A. H. & Fleming, G. J. Are encapsulated anterior glass-ionomer restoratives better than their hand-mixed equivalents? J. Dent. 37, 133–140 (2009).
[23] Fleming, G. J., Farooq, A. A. & Barralet, J. E. Influence of powder/liquid mixing ratio on the performance of a restorative glass-ionomer dental cement. Biomater. 24, 4173–4179 (2003).
[24] Zoergiebel, J. & Ilie, N. Evaluation of a conventional glass ionomer cement with new zinc formulation: effect of coating, aging and storage agents. Clin. Oral Investig. 17, 619–626 (2013).
[25] Nomoto, R., Komoriyama, M.,McCabe, J. F.&Hirano, S. Effect of mixing method on the porosity of encapsulated glass ionomer cement. Dent. Mater. 20, 972–978(2004).
[26] Arcoria, C. J., Butler, J. R.,Wagner, M. J. & Vitasek, B. A. Bending strength of Fuji and Ketac glass ionomers after sonication. J. Oral Rehabil. 19, 607–613 (1992).
[27] Xie, D., Brantley, W. A., Culbertson, B. M. &Wang, G. Mechanical properties and microstructures of glass-ionomer cements. Dent. Mater. 16, 129–138 (2000).
[28] Dowling, A. H. & Fleming, G. J. Can poly(acrylic) acid molecular weight mixtures improve the compressive fracture strength and elastic modulus of a glass-ionomer restorative? Dent. Mater. 27, 1170–1179 (2011).
[29] Dowling, A. H. & Fleming, G. J. The influence of poly(acrylic) acid number average molecular weight and concentration in solution on the compressive fracture strength and modulus of a glass-ionomer restorative. Dent Mater. 27, 535–543 (2011).
[30] Denisova, L. A., Maev, R. G., Poyurovskaya, I. ., Grineva, T. V., Denisov, A. F., Maeva, E. Y., & Bakulin, E. Y. (2004). The use of acoustic microscopy to study the mechanical properties of glass-ionomer cement. Dental Materials, 20(4), 358-363.
[31] 13. Sayers C.M., Greenfell R.L. Ultrasonic propagation through hydrating cement. Ultrasonics 1993;31:147—53.

[32] 9. Watanabe T, Miyazaki M, Inage H, Kurokawa H. Determination of elastic modulus of the components at dentin–resin interface using the ultrasonic device. Dental Materials Journal 2004;23:361–7
[33] Bar-Cohen, Y. "Nondestructive inspection and quality control." ASM International Handbook 3 (1996): 727-798.
[34] A.Shoch, ‘’the transmission of sound plane waves through plates’’, Acoustica ,2(1952) pp.1-17
[35] Brekhovskikh L M, *Waves in Layered Media*, (L M, 2nd edn New York: Academic, p 503, 1980).
[36]K. K. Phani, A.K.Maitra , Strength and elastic modulus of a porous brittle solid: an acousto-ultrasonic study, (J.Mater.Sci,29 pp. 4335-4341,1986).
[37]K. K. Phani, A.K.Maitra , ultrasonic evaluation of elastic parameters of sintered powder Compacts, (J.Mater.Sci,29, pp. 4415-4419, 1994).
[38]R. J. M. Da Fonseca and J. Attal, Elastic microcharacterization of porous materials by acoustic signature, Ph.D. Thesis, University of Montpelleir II, 1995
[39]K. K. Phani, A.K.Maitra , ultrasonic evaluation of elastic parameters of sintered powder Compacts, (J.Mater.Sci,29, pp. 4415-4419, 1994).
[40]Hartmann B. Ultrasonic measurements. Part C. In: Marton L, Marton C, editors. Physical properties. New York: Academic Press; 1980. p. 59—90. 7.
[41] Swallow GM. Ultrasonic techniques. Mechanical properties and testing of polymers, vol. 57. Dordrecht: Kluwer Academic Publishers; 1999. p. 260—4
[42] Yeheskel, O. "Nondestructive evaluation of the dynamic elastic moduli of porous iron compacts." Journal of Testing and Evaluation 32.1 (2004): 1-7.
[43]Ohdaira, E., & Masuzawa, N. (2000). Water content and its effect on ultrasound propagation in concrete—the possibility of NDE. Ultrasonics, 38(1), 546-552.
[44]I. A. Victorov, Rayleigh and Lamb waves: physical theory and applications , (Ed . Plenum Press, New York 1967).
[45]DEBBOUB Salima, Attenuation of Rayleigh Surface Waves in a Porous Material, CHIN. PHYS. LETT. Vol. 29, No. 4,044301, 2012.

9/22/2023